Colloid Polym Sci 273:279–287 (1995)
© Steinkopff Verlag 1995

ORIGINAL CONTRIBUTION

P. Sakellariou
T.A. Strivens
F. Petit

Polymer modified colloidal dispersions

Part I: Phase behaviour and interactions

Received: 8 February 1994
Accepted: 3 June 1994

P. Sakellariou[1] · T.A. Strivens
ICI Paints
Wexham Road
Slough, SL2 5DS, United Kingdom

[1]*Current address*: Dr. P. Sakellariou (✉)
New Technology Group
Courtaulds Coatings Ltd.
Stoneygate Lane
Felling, Gateshead
Tyne & Wear, NE10 OJY, United Kingdom

F. Petit
ESPCI
Laboratoire Physicochimie Structurale et Macromoleculaire
Paris, France

Abstract The effect of added polyvinyl alcohol (PVA) and polyvinyl pyrrolidone (PVP) on a dispersion of polystyrene particles stabilised with grafted methoxy PEG chains is discussed. PVA adsorbed more strongly on the particles compared to PVP. Polymer addition led to stable mixtures in the case of PVA compared to depletion phase separation observed in the case of PVP. Rheological measurements showed thickening of the dispersion and absence of any structure in the case of PVA, in contrast to structure formation in the case of PVP due to depletion phase separation. A weak gel state was reached for ca. 7% w/w PVP. The observed behaviour is in accord with the relative propensity of PVA and PVP to interact with the particle surface, the grafted chains and their solubility in water. The solvency of the free polymer chains dominated the overall behaviour while the contribution from the incompatibility between free and grafted chains was counterbalanced by differences in the free polymer adsorption on the particles.

Key words Colloidal dispersion – polymer – particles – interactions – phase diagram – depletion – phase separation – rheology – structure

Introduction

The effect of added polymer on the phase behaviour and rheology of colloidal dispersions has been the subject of extensive research in both academe [1] and industry [2], with several excellent critical reviews [3]. Sperry and coworkers [5] have used the Asakawa and Oosawa [6, 7] volume restriction theory to calculate the potential energy curves of polymer-modified aqueous polymer colloids. More importantly, they attempted to correlate floc morphology with sedimentation behaviour. Dey and Hirtzel [8] calculated the phase diagrams of colloidal dispersions, aqueous and non-aqueous, with added non-adsorbing polymers using an exact calculation of the radial distribution function. In agreement with other workers [9], they identified two important parameters for the control of phase behaviour, namely the polymer concentration and the ratio of polymer coil dimension to that of the particle. They concluded that, in aqueous systems the dependence of phase behaviour on polymer concentration was very weak; higher polymer concentration and larger polymer sizes are prerequisite to flexible control of phase behaviour. The effect of size of the polymer coil on the phase behaviour has also been the subject of a number of experimental [10] and theoretical [11] works.

Scheutjens and Fleer [12–16], have developed a comprehensive theory for the interaction between hard and soft surfaces (hairy surfaces) in the presence of free adsorbing and non-adsorbing polymer. The interactions are accounted for by the osmotic pressure differential, giving rise to attraction, as two particles approach each other and free polymer is excluded from the gap between them. When the grafted polymer layers start to overlap considerably, a strong repulsive force is generated. In the case of soft spheres, there is an additional entropic term due to interaction between hairs which can give rise to attractive or repulsive potentials. Their theory allowed treatment of the effect of interaction between free and grafted polymer chains and solvency [12]. The model predicts that when polymer miscibility decreases the interpenetration of free polymer and grafted layer diminishes leading to larger depletion layer thickness and hence stronger attraction. They concluded that free polymer/grafted polymer miscibility is often the dominant factor in the case of changes in solvency. When free and grafted polymers are of the same type, solvency may play a role.

We discuss the interactions and phase behaviour of hairy polystyrene particles stabilised with methoxy-terminated polyethylene oxide chains covalently attached to the particle surface, in the presence of free polymers different to the stabilising species. The free polymers were polyvinyl alcohol and polyvinyl pyrrolidone. The strength of the interactions has been evaluated by means of surface energy and rheology measurements and discussed in terms of the observed phase behaviour. These observations have been used to explain the solid state morphology of the same systems in Part II of this paper.

Materials and methods

Aqueous dispersion

The aqueous dispersion was a polystyrene (PS) latex prepared by a seed and feed two-stage process in the presence of ethanol which helps solubilise the monomer. Particles were stabilised by a reactive stabiliser, methoxy PEG2000 methacrylate (MeOPEG2000MA, 45 ethylene oxide units). Ethanol was distilled off and remaining unreacted species were removed by six consecutive cycles of centrifugation – decantation – redispersion at 14000 rpm. The particle size, measured by photon correlation spectroscopy (Malvern Autosizer 2), was 445 nm.

Polymers

Poly(vinyl alcohol), PVA Poval 205, supplied by Kuraray Ltd, was 88% hydrolysed with viscosity of 4.6–5.4 cps in 4% aqueous solutions at 20 °C. The molecular weight was $\bar{M}n = 73{,}900$ and polydispersity index of 1.7. Poly(vinyl pyrrolidone), PVP K90 GAF, had an intrinsic viscosity of 1.5 cps and $\bar{M}n$ of 187,000 with a polydispersity of 5.3. Molecular weights and polydispersities were determined by gel permeation chromatography (GPC) with tetrahydrofuran as the carrier solvent and polystyrene standards.

Surface energy measurements

The surface energy was determined from the contact angle of three probe liquids: water, glycerol and *n*-hexane. Contact angles were determined by means of the Dynamic Contact Angle Analyser (DCA 312, Cahn Balance) which is based on the Willhelmy plate principle [17]. Contact angles were measured on polymer films coated on microscope cover slips and dried at room temperature overnight. Residual solvent was removed under vacuum 90 °C.

Adsorption isotherms

Adsorption isotherms were determined by allowing blends of latex and polymer at different and known concentrations to stand for 2 days to reach equilibrium. The latex particles were separated from the blend by careful centrifugation (14000 rpm for 2 h) and a sample of the supernatant solution was carefully removed and weighed. The polymer concentration in the supernatant was measured by appropriate spectroscopic methods depending on the polymer. Isotherms are reported as weight of polymer adsorbed per unit surface area of the particles (A) against polymer concentration in the blend.

PVP analysis was based on the single band in the 190–200 nm region due to $\pi \rightarrow \pi^*$ excitation of the carbonyl electrons [18]. According to Beer-Lambert law, the absorbance at 196 nm is proportional to the weight concentration of PVP in the solution. A calibration curve was constructed by measuring the absorbance of PVP solutions of known concentration by means of SP8-150 UV/V is spectrophotometer and quartz cells.

The PVA concentration was determined by spectrophotometric measurements of the absorbance at 690 nm of iodide complexes of the polymer in the presence of boric acid [19]. A calibration curve was constructed from a PVA stock solution and a reference solution of boric acid and iodine solution diluted with deionised water. Care was taken to maintain polymer concentration within the linear region of the calibration curves.

Rheological measurements

Viscosity-shear rate measurements were obtained at 25 °C using a Bohlin VOR rheometer, equipped with 3 cm-diameter 1 degree cone/plate geometry. Measurements of the dynamic elasticity modulus were also made at 25 °C, using a Carrimed CSL 100 controlled stress rheometer, provided with 6 cm-diameter 2° cone/plate geometry. Sample/air interfaces in the measuring geometries were protected by solvent traps to prevent drying. Measurements of modulus were made at fixed low and high frequencies as a function of stress amplitude, in order to determine the limit of linearity (modulus independent of amplitude). Measurements of modulus against frequency were carried out at stress amplitudes below the linearity limit.

Phase diagrams

Blends with latex contents in excess of 5% were allowed to demix at ambient temperature in 100 ml test tubes sealed to avoid water evaporation and contamination. The number of phases and their relative volume were monitored with time. Equilibrium was judged to have been achieved when there was no detectable change in the phase boundaries in three consecutive days. Blends with latex contents below 5%, were studied by spectrophotometric measurements with varying wavelength [18, 19] with an SP8-150 UV/Vis spectrophotometer, from 400 to 650 nm.

Results and discussion

Lewis acid-base interactions and polymer adsorption

The adsorption isotherms (Fig. 1) show clearly that PVA adsorbs more strongly on the PS particles than PVP. The same data indicate that the initial slope of the adsorption isotherm for PVP is higher than that of PVA, suggesting perhaps a stronger adsorption of PVP at very low polymer concentration. The adsorption behaviour of the polymers is related to the relative strength of their interactions with water, the particle surface and MeOPEG grafts.

We have investigated these interactions by means of the Lewis acid-base concept [22]. The surface energy can be conveniently split into a dispersive part (σ^d) reflecting the London-van der Waals forces, a Lewis acid part (σ^+) and a Lewis base part (σ^-). These were determined from the contact angles of three probe liquids on the polymer. The contact angle (θ_H) of n hexane yields the dispersive component from:

$$\sigma_2^d = \sigma_H(1 + \cos\theta_H)/4 \; . \tag{1}$$

For the remaining two components, a system of two equations was constructed:

$$(1 + \cos\theta_w)\sigma_w = 2\sqrt{\sigma_2^d \sigma_w^d} + 51\delta_{2W}^+ + 51\delta_{2W}^- \tag{2}$$

$$(1 + \cos\theta_G)\sigma_G = 2\sqrt{\sigma_2^d \sigma_G^d} + 63.5\delta_{2G}^+ + 24\delta_{2G}^- \tag{3}$$

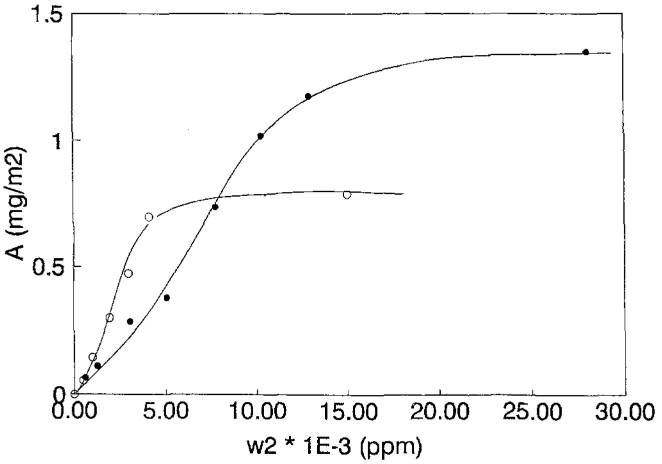

Fig. 1 Adsorption isotherms of PVA (●) and PVP (○) on the PS latex

Where:

$$\delta_{2W}^+ = \sqrt{\sigma_2^+/\sigma_W^+} \tag{4}$$

$$\delta_{2W}^- = \sqrt{\sigma_2^-/\sigma_W^-} \tag{5}$$

$$\delta_{2G}^+ = \sqrt{\sigma_2^+/\sigma_G^+} \tag{6}$$

$$\delta_{2G}^- = \sqrt{\sigma_2^-/\sigma_G^-} \; . \tag{7}$$

The remaining two unknowns, σ_2^+ and σ_2^-, of the system of Eqs. (2) and (3) were obtained by a simple elimination procedure. Table 1 summarises the experimentally determined values together with literature data for polyethylene oxide (PEO). PVA and PVP had similar dispersive components but different Lewis acid and base components, with PVA being stronger Lewis base and weaker Lewis acid than PVP. The stronger amphoteric nature of PVA would encourage Lewis acid-base interactions with the other species in the colloidal system. We can now calculate the polymer-solvent interaction parameters, χ_{12}:

$$\frac{\chi_{12}kT}{S_c} = 2(\sqrt{\sigma_2^d} - \sqrt{\sigma_w^d})^2 - 4(\sqrt{\sigma_2^+\sigma_2^-} + \sqrt{\sigma_W^+\sigma_W^-} - \sqrt{\sigma_W^+\sigma_2^-} - \sqrt{\sigma_W^-\sigma_2^+}) \; , \tag{8}$$

where S_c is the cross-sectional surface area for polymer-polymer interactions, calculated from the diameter of the polymer reptation tube by means of computer molecular modelling. The polymer-solvent interaction parameter for PVA was significantly lower than that for PVP (Table 1), the latter existing in a nearly theta solvent; both parameters were significantly higher than that of PEO. Everything else being equal, the polymer chains will be increasingly expanded as we move from PVP to PVA and,

Table 1 Dispersive, Lewis acid and base contributions to the surface energy, χ_{12} interaction parameters and partial solubility parameters for PVA, PVP and PEO

Polymer	dyne/cm σ_2^d	σ_2^+	σ_2^-	χ_{12}	δ_d	MPa$^{1/2}$ δ_p	δ_h
PVA	18.4	1.0	13.1	0.26	16.4	14.7	24.2
PVP	18.4	1.5	9.1	0.51	12.5	22.3	0.0
PEO*	43		64	> − 2.78	17.5	10.0	9.4
PS	42		1.1	21.3	5.8	4.3	
MeOPEG-2000MA				16.6		10.4	8.4

finally, PEO. Table 1 also shows the Hansen solubility parameters (δ) [21] for the different components of our systems calculated from Hoy's groups contribution constants [22].

The solubility parameter of MeOPEG2000MA was based on the chemical structure of the stabilizer alone ignoring the polystyrene backbone, inadvertently present in the final system. The solubility parameters have been used to calculate the polymer-polymer interaction parameters by means of a van Laar-type expression [23]:

$$\chi_{ij} = \frac{V(\delta_1 - \delta_j)^2}{RT}\,, \tag{9}$$

where V is the polymer molar volume. Table 2 summarises the χ_{ij} values for the dispersion polymer (1), free polymer (2) and stabilizer MeOPEG2000MA (s). Note that polymer-stabiliser and polymer-particle interaction parameters are lower for PVA than PVP. This is taken as an indication that the former has a higher affinity for the particle and stabiliser compared to the latter. This is consistent with the increased adsorption of PVA on the particles illustrated by the adsorption isotherms of Fig. 1.

Table 2 Polymer-polymer interactions calculated from Eq. (9) 1 = particle; 2 = free polymer; s = stabiliser

Polymer	χ_{1s}	χ_{2s}	χ_{12}
PVA	0.06	0.41	0.16
PVP	0.06	0.74	0.38

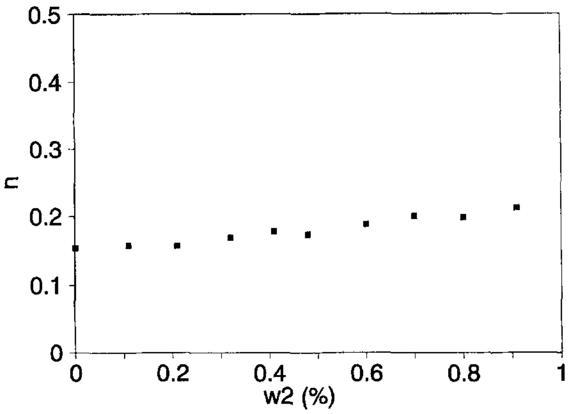

Fig. 2 Variation of parameter n with added PVA weight fraction; $w1 = 0.01$

Phase diagrams

Blends with less than 0.5% w/w polymer were studied by UV-vis spectrophotometry. A plot of log OD (OD = optical density) against log λ (λ = wavelength) is expected to be a straight line [23, 24] with a slope equal to a parameter n which relates to the particle size.

Parameter n equals 4 for particles much smaller than the light wavelength; for larger particles it decreases and eventually oscillates around zero [24, 25]. The data suggest that no significant change in the particle stability takes place with addition of up to ca. 1% PVA into the dilute polymer dispersion ($\phi_1 < 0.05$), the particle size remaining below that of the visible light wavelength (560 nm) (Fig. 2). Addition of polymer in more concentrated polymer dispersion led to stable mixtures, consistent with increased stabilisation of the particles through PVA adsorption. Addition of PVP to a dilute polymer dispersion ($\phi_1 < 0.05$) produced also a stable system with particle size below that of the visible light. However, its incorporation into the concentrated system resulted in depletion phase separation (Fig. 3) leading to formation of a particle-rich phase and a particle-depleted phase, in accord with theoretical predictions and observations on the effect of non-adsorbing polymers on polymer colloids.

Rheology

Two types of measurements were made: dynamic (oscillatory) and steady state. The dynamic measurements were expected to probe the presence of structure due to component interactions, whilst the steady-state measurements (viscosity-shear rate) yield information on structure breakdown. Because of the likelihood of such structure being

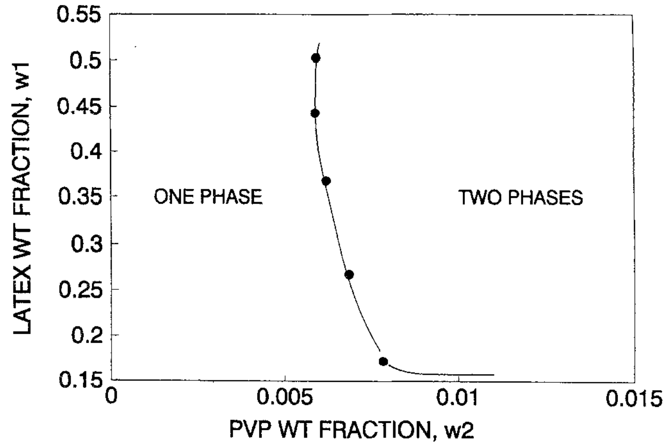

Fig. 3 Phase diagram for the PVP/latex blend after 166 h

weak, care was taken to choose stress amplitudes within the linear response region for dynamic measurements.

The dynamic data for the latex alone (Fig. 4) was typical of a latex of this particle size and concentration. Whilst some elasticity was observed at the high frequency end, the modulus value was small. In spite of noise at the high frequency end on both the elasticity and loss modulus vs frequency plot, the main features of a sharp transition between viscous and elastic behaviour were observable. A cross-over ($G' = G''$) was observed at about 5 Hz, whilst the terminal slopes of the double logarithmic plots at the lowest frequencies were approximately unity for the loss modulus (G'') and two for the elasticity modulus (G'). This behaviour is typical of a single relaxation time. The values of G'' at the low frequency end correspond to an approximately constant dynamic viscosity value (η') of 0.016 Pas. This is in good agreement with the value of 0.014 Pas averaged from the approximately Newtonian viscosity values of the steady state measurements over a shear rate range of 80–2000 s^{-1}. Calculation of the particle radius, using the Stokes-Einstein equation for the relaxation time value from the approximate cross-over frequency of 5 Hz, yields a value of 0.2 μm, in accord with the value of 0.223 μm measured by the Malvern Autosizer. Over the same shear rate range, the PVP and PVA solutions showed Newtonian viscosities of 0.088 Pas and 0.369 Pas, respectively.

In the PVA modified latex, shear rate dependency decreased and low shear rate (Newtonian) viscosity increased with increasing polymer content (Table 3). Typical viscous liquid behaviour was observed (Fig. 5), with the loss modulus (G'') above the elasticity modulus (G') over the whole frequency range scanned. The log G'' versus log frequency plot was a straight line of slope unity. Plots of moduli against shear stress amplitude showed no dependence on amplitude even at very low stress amplitudes (< 0.1 Pa), indicating the absence of even the weakest structure in the polymer/latex blends. The viscosity increase observed is partly due to an increase in total phase volume of the particles, resulting from adsorption of the PVA onto the particle surface and consequent increase in the effective total diameter of the particle (core plus stabiliser layer). This could also give rise to the small amount of pseudoplasticity evident at the lowest PVA concentration.

The rheology of the latex/PVP mixtures was in considerable contrast with that of the PVA systems. Whilst a small addition of PVP to the latex produced little change beyond that expected of slight dilution of the latex, further additions lead to considerable changes in the rheology of the mixture. The system with 0.15% PVP had a Newtonian viscosity of 0.014 Pas over the shear rate range 1270–2000 s^{-1} (cf. undiluted latex 0.016 Pas) (Fig. 6). The dynamic data (Fig. 7) showed a viscous liquid response. The system with 0.46% PVP exhibited strong shear rate

Fig. 4 Variation of G' (●) and G'' (○) with frequency f(Hz) for the latex

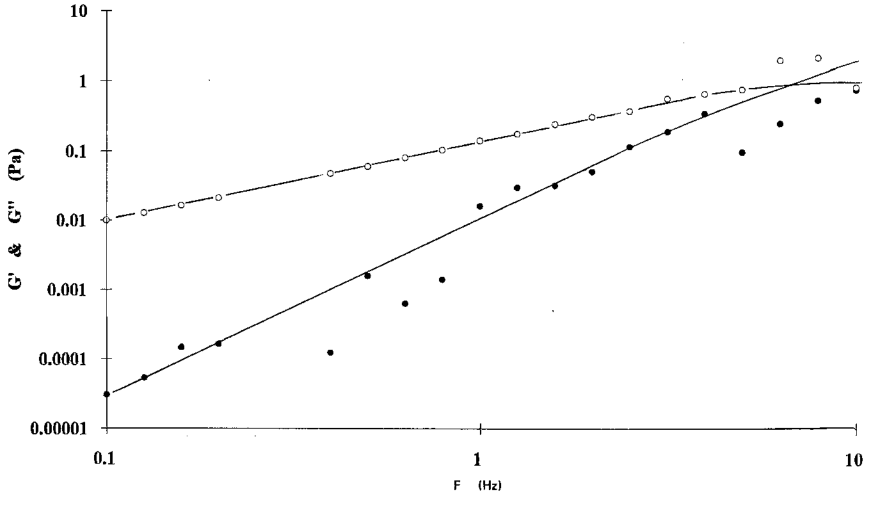

Table 3 Viscosity values for PVA/latex mixtures (continuous shearing)

Latex wt%	Polymer wt%	Low shear rate η (poise)	High shear rate η (poise)
53.6	–	0.14	0.14
41.2	4.6	2.12	1.27
21.4	12.0	2.40	2.25
9.0	16.7	3.31	3.13
–	20.1	3.69	3.69

dependence in the steady data, with the viscosity falling steeply from 0.090 Pas at 20 s^{-1} and levelling off at around 2000 s^{-1} shear rate at a value of 0.014 Pas. The dynamic data now showed strong stress amplitude dependence beyond a value of 0.4 Pa and, although the frequency sweep showed predominantly viscous behaviour, the slope of the G'' plot was less than unity. This blend showed even greater shear rate dependency in the steady state data with some time dependency (thixotropy) evident. Thus the viscosity dropped from 6.4 Pas at 0.8 s^{-1} to 0.62 Pas at 2000 s^{-1} shear rate. The high shear rate viscosity was increasingly dominated by the PVP solution viscosity. Even at this low shear rate (0.8 s^{-1}), there was no evidence of flattening off to a Newtonian plateau value. In the dynamic data, the linear response region became more extensive than the 0.46% PVP blend with the moduli values falling sharply at stress amplitudes greater than 1.1 Pa. The frequency scan now showed a strong increase in both moduli values and a cross-over close to 5 Hz, with the shape of the G'' plot suggesting a wide relaxation time range and, at low frequency, slope of double logarithmic plot less than unity. The mixture with 7.4% PVP was characterised by a much more complete structure than the previous mixture, but much lower in strength. The dynamic data showed weaker structure: the moduli values showed strong decreases for stress amplitudes greater than 0.12 Pa. By contrast, G' was independent of the frequency

Fig. 5 Dynamic data for PVA/latex blends (a) G'; (b) G'' (■) 0% PVA; (●) 4.6% PVA; (○) 12% PVA; (△) 16.7% PVA

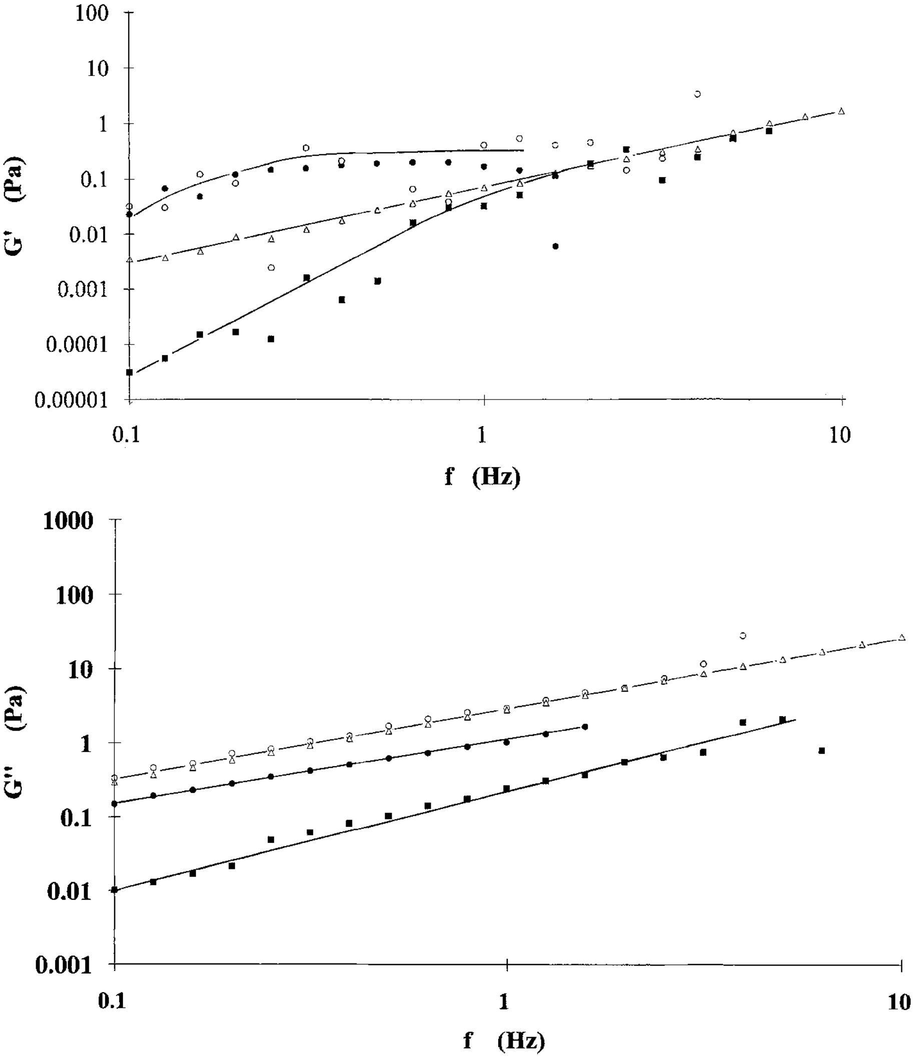

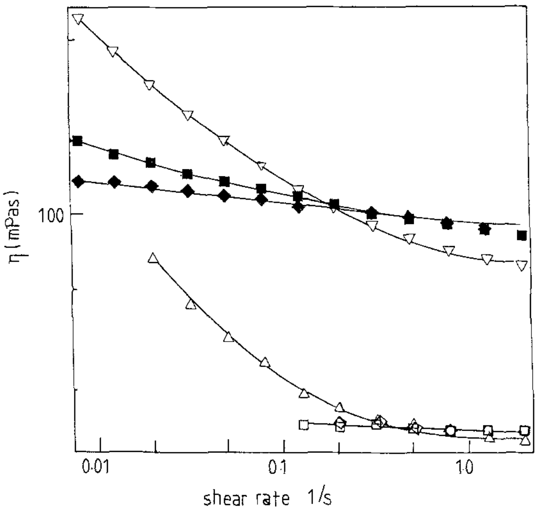

Fig. 6 Viscosity versus shear rate for PVP/latex mixtures 0% PVP (□); 0.2% PVP (◇); 0.5% PVP (△); 4.0% PVP (▽); 7.4% PVP (■); 9.0% PVP (◆)

and an order of magnitude greater than G''. The G' value was similar to the maximum high frequency value for the previous mixture. The viscosity shear rate data confirmed this picture, as the viscosity dropped steadily from 0.2 Pas at 8 s^{-1} to 0.08 Pas at 2000 s^{-1} shear rate without any levelling off at the high shear rate end (cf. the previous mixture showed values of 0.55–0.06 Pas over the same shear rate range).

Again, an increase in the high shear rate viscosity results from the increase in polymer solution content. The final mixture (8.95% PVP) showed a further sharp change. At low shear rates (around 10 s^{-1}), a Newtonian plateau value of 0.12 Pas was evident. The viscosity value then started to show some shear rate dependency as shear rate was increased, until a value of 0.08 Pas was reached at 2000 s^{-1}. The moduli values were independent of stress amplitudes up to values of 1 Pa, whilst the frequency sweep showed typical viscous liquid behaviour with the loss modulus greater than the elasticity modulus over the whole frequency range measured.

Our rheology studies have shown that small additions of PVP lead to latex dilution indicated by the disappearance of the feeble viscoelasticity observed with the undiluted latex (Fig. 4) and the liquid-like Newtonian viscosity-shear rate behaviour (Fig. 6). Further addition of polymer to the latex, in spite of dilution of the latex, produced increasing levels of structure formation, resulting from latex flocculation. This is shown by increasing shear rate dependence of the viscosity and increasing values of the dynamic elasticity modulus over the whole frequency range as the PVP content increases. The studies on phase separation suggest that structure formation is due to depletion or bridging flocculation of the particles by the polymer with a complete network or weak 'gel' state reached at the 7.4% PVP level. At the highest (9.0%) and lowest PVP level (0.4%), the absence of significant viscoelasticity (in particular, low G' values) suggest depletion rather than bridging flocculation as the mechanism responsible for structure formation.

The picture was completely different for the PVA systems. The elasticity modulus remained low and did not differ significantly from that of the undiluted latex. The loss modulus plots remained parallel but increased in value with increasing polymer concentration. For the last two concentrations, the values are virtually the same. The increase in the loss component was consistent with the viscosity of the continuous phase increasing with polymer concentration. The diminution of the overall mixture viscosity is probably due to a reduced contribution from the latex phase volume, as the latex is diluted by polymer addition. The corresponding increase in cross-over frequency as the latex content decreases merely reflects the increasing dominance of the viscoelastic response of the mixture by the dynamic properties of the polymer solution. This implies that in a polymer modified latex system as much as in an undiluted latex, the viscoelastic properties of the whole are only affected by the latex, within the frequency range used for the measurements. This is true only if the latex concentration is above a certain limiting value, such that the particles are on average close enough to affect each other's motion. Naturally, if there is interaction between the particles and the polymer, this limiting latex concentration has a lower value. This is because the effective particle size becomes that of the latex/polymer flocs, formed by the interaction forces. Consequently, the effective disperse phase volume becomes that of the flocs, rather than of their constituent latex particles, and the flocs are close enough in space to hinder each other's motion.

From the dynamic data (Fig. 7), it can be seen that with the exception of the systems with the minimum and maximum PVP content, the high frequency elasticity values are going to level off at values considerably in excess of the latex value (19 dyne/cm^2), indicating the presence of considerable interaction/structure in such mixtures. By contrast (Fig. 5), the values of the PVA mixtures are much lower and around or less than the latex value, indicating the sole contribution of the latex to the viscoelasticity of the PVA/latex mixtures. The steady-state viscosity-shear rate confirmed this: the PVA mixtures showing a smaller shear rate dependence and overall increasing viscosity values as the PVA content increased.

By contrast, the PVP solution/latex mixtures showed the same increases in viscosity due to increasing polymer content but at high shear rate only. The low shear rate

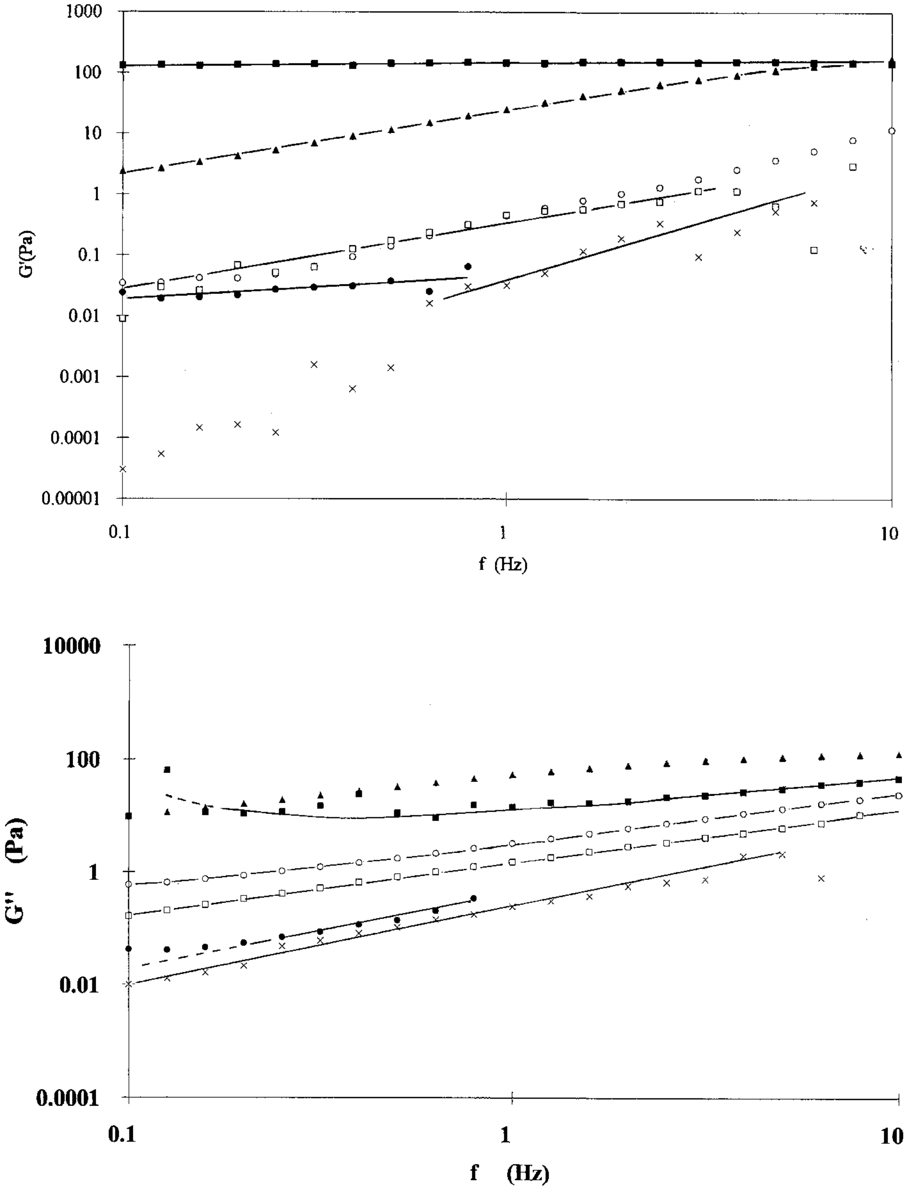

Fig. 7 Dynamic data for PVP/latex blends (a) *G'*; (b) *G"* (×) 0% PVP; (●) 0.2% PVP; (○) 0.5% PVP; (▲) 4% PVP; (■) 7.4% PVP; (□) 9.0% PVP

data showed increasingly the effects of interaction/structure formation between the polymer and the latex components, until there was insufficient latex to form structure and the shear rate dependence over the whole range measured becomes small again as for the PVA/latex mixtures.

General discussion

We have investigated the interactions of two free polymers with the particle surface, the grafted polymer chains and the continuous phase (water) in polymer modified colloids. PVA showed higher propensity for interactions with both the MeOPEG grafts and the PS particle bare surface. The same polymer existed in a good solvent compared to PVP which was in a theta solvent. The magnitude of the particle-particle interaction energy potential, $A_{\min}$ is given by [12]:

$$A_{\min} = -2\pi a \prod \Delta^2 , \qquad (10)$$

where a is the diameter of the particle, Π is the osmotic pressure difference between the bulk solution and the interparticle gap and Δ is the depletion layer thickness. As the free polymer-solvent interaction parameter χ_{20} increases, the osmotic pressure decreases giving rise to a stronger attraction between particles. At the same time, the degree of overlap between free and grafted chains decreases since the free polymer chains assumed an increasingly collapsed conformation in solution; this leads to an increase in the depletion layer thickness and a deeper interaction minimum. This contribution would dominate the overall behaviour leading to increased interparticle attraction in the case of PVP ($\chi_{20} = 0.26$) compared to PVA ($\chi_{20} = 0.51$). The next contribution is due to changes in the miscibility between free and grafted chains. Increasing incompatibility between the free polymer and the MeOPEG grafts would reduce their overlap leading to bigger Δ values and hence deeper interaction minima.

This contribution would predict increased particle attraction for the PVA system compared to the PVP one. The experimental observations suggest that PVP produces deeper interaction minima compared to PVA leading to depletion phase separation. The implication is that the solvency of the free polymer contribution dominated the overall behaviour of our systems. Perhaps the opposing contribution of the (in)compatibility between free and grafted chains was also counterbalanced by increased absorption of PVA compared to PVP, leading to enhanced particle stability, in the first instance, and altering the effective depletion layer thickness. Adsorption of PVA on the bare particle surface and on the steric sheath would introduce some additional degree of flexibility enhancing polymer overlap and depressing the attraction between particles. Such adsorption process for PVA would be in agreement with our rheology observations suggesting thickening of the dispersion through thickening of the continuous phase and an increase in the apparent volume fraction through increases in the apparent particle diameter. On the other hand, the gel structure observed for a range of PVP concentrations would be a product of continuous network formation involving the free polymer and particle flocs. In Part II of this paper, we will attempt to correlate these observations to the solid state morphology of these blends.

References

1. Jones A, Vincent B, Colloids Surf (1989) 42:113–128; *ibid* (1990) 50:241–249
2. Sperry PR, J Colloid Interface Sci (1981) 82:62; *ibid* (1981) 87:375; *ibid* (1984) 1:97–108
3. Tadros, Th F (Ed.) (1982) In: The Effect of Polymers on Dispersion Properties, AP, London
4. Tadros, Th F (Ed.) (1987) In: Solid/Liquid Dispersions, AP, London
5. Sperry PR, Thibeault JC, Kostansek EC, 1–11
6. Asakura S, Oosawa F (1954) J Chem Phys, 22:1255–1256
7. Asakura S, Oosawa F (1958) J Polym Sci, 33:183–192
8. Dey D, Hirtzel CS, Colloid Polym Sci (1991) 269:28–35
9. Russel WB, Saville DA, Schowalter WR (1989), in Colloid Dispersions, 328–364, Cambridge University Press, Cambridge
10. Gast AP, Hall CK, Russel WB (1983) J Colloid Interface Sci, 96:251–267
11. Gast AP, Russel WB, Hall CK, Faraday Disc (1986) 76:189–171
12. van Lent B, Israels R, Scheutjens HM, Fleer GJ (1990) J Colloid Interface Sci 137:380–394
13. Scheutjens HM, Fleer GJ (1979) J Phys Chem 83:1619–1635
14. Scheutjens HM, Fleer GJ (1980) J Phys Chem 84:178–190
15. Scheutjens HM, Fleer GJ (1982) Adv Colloid Interface Sci 16:341–359
16. Scheutjens HM, Fleer GJ (1987) Croatica Chem Acta 60:447–494
17. Sakellariou P (1993) Polymer 34:3408–3415
18. Cohen Stuart MA (1980), in Flexible Polymers at a Solid-Liquid Interface, PhD Thesis, Arnhem
19. Finley JH, Anal Chem (1965) 33:1925–1928
20. Van Oss CJ, Arnold K, Good RJ, Gawrisch K, Ohki SJ, J Macromol Sci Chem A (1990) 27:563–569
21. Hansen CM, J Paint Technol (1967) 39:104–117
22. Hoy KL, J Paint Technol (1970) 42:76–118
23. Sakellariou P, Hassan A, Rowe RC, Polymer (1993) 34:1240–1248
24. Long JA, Osmond DW, Vincent B (1973) J Colloid Interface Sci, 42:545–553
25. Heler W, Bhatnagar HL, Nakagaki M, J Chem Phys, 36:1163–1170